HHS Public Access

Author manuscript

J Neurochem. Author manuscript; available in PMC 2017 November 01.

Published in final edited form as:

J Neurochem. 2016 November ; 139(3): 432–439. doi:10.1111/jnc.13771.

Mapping the alterations in glutamate with GluCEST MRI in a mouse model of dopamine deficiency

Puneet Bagga[1,*], **Rachelle Crescenzi**[1,*], **Guruprasad Krishnamoorthy**[1], **Gaurav Verma**[1], **Ravi Prakash Reddy Nanga**[1], **Damodar Reddy**[1], **Joel Greenberg**[2], **John A. Detre**[3], **Hari Hariharan**[1], and **Ravinder Reddy**[1]

[1]CMROI, Department of Radiology, University of Pennsylvania, Philadelphia, PA, United States

[2]Department of Neurology, University of Pennsylvania, Philadelphia, PA, United States

[3]Center for Functional Neuroimaging, Department of Neurology, University of Pennsylvania, Philadelphia, PA, United States

Abstract

Glutamate Chemical Exchange Saturation Transfer (GluCEST) MRI was used to measure metabolic changes in mice treated with 1-methyl-4-phenyl1,2,3,6-tetrahydropyridine (MPTP) by mapping regional cerebral glutamate. The GluCEST contrast following MPTP treatment was correlated with ^{1}H MR spectroscopy, motor function and immunohistochemical measures. GluCEST contrast was found to be significantly higher in the striatum and motor cortex of mice treated with MPTP than in controls ($p<0.001$), which was confirmed by localized ^{1}H MR spectroscopy. Elevated striatal GluCEST was positively associated with local astrogliosis measured by immunohistochemistry for glial fibrillary acidic protein (GFAP). Additionally, a negative correlation was found between the GluCEST of striatum ($R = -0.705$, $p<0.001$) and motor cortex ($R = -0.617$, $p<0.01$) with motor function measured by the four limb grip strength test, suggesting a role of elevated glutamate in the abnormal cerebral motor function regulation. GluCEST contrast and GFAP staining were unaltered in the thalamus indicating glutamate elevation was localized to striatum and possibly motor cortex. These findings suggest that in addition to measuring spatial changes in glutamate, GluCEST may serve as an *in vivo* biomarker of metabolic and functional changes that may be applied to the assessment of a broad range of neuropathologies.

Keywords

Glutamate; Astrogliosis; Brain; GFAP; MRI; CEST; Tyrosine hydroxylase

Corresponding Author: Ravinder Reddy PhD, CMROI, Department of Radiology, University of Pennsylvania, Philadelphia, PA, United States. Tel: 215-898-5708. Fax: 215-573-2113. krr@upenn.edu.

*These authors contributed equally

Conflict of Interest

The authors declare no conflict of interest

Introduction

Parkinson's disease (PD) is the second most common neurodegenerative disorder. PD is caused by the loss of dopaminergic neurons in the substantia nigra pars compacta (SNc) leading to diminished level of dopamine (DA) in the basal ganglia. The basal ganglia functions to control the movement via the cortico-striatal-thalamo-cortical dopaminergic pathway also known as nigrostriatal pathway and the loss of the dopamine in basal ganglia leads to inadequate motor control (Alexander 1994). Clinical manifestations of PD include symptoms such as bradykinesia, esting tremors and muscular rigidity (Gazewood *et al.* 2013, Obeso *et al.* 2000). Currently, PD is diagnosed based on these motor symptoms which occur after the loss of 50–90% DA in the striatum (Kordower *et al.* 2013).

We used the 1-methyl-4-phenyl1,2,3,6-tetrahydropyridine (MPTP) induced dopamine deficient parkinsonism mouse model, which exhibits localized substantia nigral dopaminergic neuronal loss with acute and chronic treatment (Gluck *et al.* 1994, Scotcher *et al.* 1990), causing a long-term astrogliosis in the striatum (Hirsch & Hunot 2009, Tristao *et al.* 2014). Elevated level of glutamate following the treatment with MPTP in the striatum are also reported, in addition to the motor function disturbances in mice (Bagga *et al.* 2013, Sedelis *et al.* 2000, Chassain *et al.* 2013). While ^{1}H MR spectroscopy is widely used to measure glutamate and other metabolites, it is beset by low spatial resolution and longer acquisition times. A recently developed method Glutamate Chemical Exchange Saturation Transfer (GluCEST) MRI technique (Cai *et al.* 2012, Kogan *et al.* 2013) enables the indirect detection of glutamate *in vivo* by measuring the metabolite effects on bulk water, thus providing greater sensitivity and spatial resolution than conventional ^{1}H magnetic resonance spectroscopy (^{1}H MRS) techniques. GluCEST imaging has previously demonstrated glutamate deficits in mouse models of dementia (Crescenzi *et al.* 2014, Haris *et al.* 2013) and epilepsy in human patients (Davis *et al.* 2015).

In this study, we evaluated the potential of GluCEST MRI as an imaging biomarker for metabolic and functional changes in a mouse model of dopamine deficiency caused by MPTP. We hypothesized that motor function derangements caused by the MPTP exposure are associated with the early changes in the glutamate levels in the striatum and motor cortex, which can be imaged with the GluCEST MRI. Behavioral, GluCEST, ^{1}H MRS and immunohistochemical measurements were performed in the MPTP treated mice two days after treatment cessation and compared with the data in age matched control mice treated with saline. Specifically, striatal glutamate changes measured by GluCEST and ^{1}H MRS were compared with the astrogliosis measured by GFAP immunohistochemistry. In addition, behavioral testing revealed changes in motor function before and after treatment of these mice, which were correlated with the changes in GluCEST contrast in both the motor cortex and striatal regions of the two groups. Potential of GluCEST as a biomarker for measuring inflammation mediated gliosis and motor function changes is discussed.

Materials and Methods

MPTP administration and animal care

The IACUC of the University of Pennsylvania approved all the experimental protocols in this study. Male C57BL6 mice were procured from the Charles River Laboratory, Horsham, PA, USA and kept at the ULAR animal housing facility at the University of Pennsylvania. Mice were housed in a humidity controlled room ~22°C under a 12 hour light/ dark cycle with *ad libitum* access to food and water. Mice aged 3 months old were divided into two groups: control (n=11) and MPTP (n=13). Mice in the MPTP group received MPTP (25 mg/kg, via intraperitoneal injection, Sigma/Aldrich, St. Louis, MO, USA) dissolved in normal saline once a day for 7 days, while the control mice received the same volume of normal saline for the same period.

Neurobehavioral testing

Forepaw grip strength test was performed on both groups of mice on the 0^{th} and 8^{th} days of treatment using a device described previously (Bagga & Patel 2012). Briefly, mice were made to hold a horizontal rod using their fore-limbs and their tail was restrained to prohibit the use of hind limbs. The duration of hanging on the rod was monitored for both groups of animals. The forepaw grip strength was measured as the holding impulse (weight × duration of holding) in order to normalize the effect of different mass of the mice.

The four limb hanging test was performed on both groups of mice on the 8^{th} day of treatment. The testing procedure implemented here was modified from a protocol previously described (Hosaka *et al.* 2002). The mice were placed on the top of a standard wire cage lid and were made to hold for a few seconds before turning the lid upside down. The latency of mice to fall off the wire lid was measured. The trial was repeated 3 times and the average value was computed. The four limb endurance was reported as holding impulse (holding impulse = weight × duration).

Acquisition and processing of anatomic MRI, ^{1}H MRS and GluCEST MRI

All spectroscopy and imaging studies were performed on a 9.4T small-animal spectrometer using a horizontal bore magnet fitted with a 12 cm gradient insert and interfaced to a Varian MR spectrometer (Agilent Technologies Inc., Santa Clara, CA). Mice were anesthetized using 1.5–2% isoflurane mixed with O_2 at 1 L/min, and secured to a body-bed inside a 20mm diameter volume coil (M2M Imaging Corp., Cleveland, OH). Body temperature was monitored using a rectal temperature probe and maintained at 37 °C using warm air blown inside the bore of the magnet.

^{1}H MR spectra were acquired from a voxel localized in the striatum (2.25×2.25×2.25 mm^3) in control (n=11) and MPTP treated (n=13) mice using the Point RESolved Spectroscopy (PRESS) pulse sequence (TR/TE=3000/28 ms, spectral width=4 kHz, number of points=4006, WET water suppression, averages=256). Another spectrum was acquired without water suppression to obtain the water reference signal for normalization (averages=16). Metabolite concentrations measured by *in vivo* ^{1}H MRS were quantified using the LCModel software (Provencher 1993). The concentration of metabolites was

measured using the unsuppressed water peak as a concentration standard. LCModel uses a least-squares algorithm to fit metabolite peaks to a prior-knowledge basis set and measures concentration using the unsuppressed water peak as a reference. Confidence in the fit was expressed in terms of the Cramer-Rao Lower-bounds (CRLB), and good fits were considered to be those with CRLBs under 20% of the standard deviation (%SD).

GluCEST, B_0, and B_1 maps were acquired from 2 coronal slices (2mm thick). One slice included the striatum and the second slice included the thalamus region. GluCEST images were acquired using a custom-programmed pulse sequence with a frequency selective saturation preparation pulse comprised of four square pulses each with a duration of 250 ms with < 10 μs delay between them (duty cycle 100%) at peak B_1 of 250 Hz (5.87 μT) for the offset frequencies ±2.5, ±2.75, ±3, ±3.25, ±3.5 ppm from the water signal at 4.7 ppm, followed by a spoiled gradient echo (GRE) readout. The sequence parameters were as follows: Field of view = 20×20 mm^2, Slice thickness = 2 mm, Matrix size = 128×128, Flip angle = 15°, GRE readout TR = 6.2 ms, TE = 2.9 ms, Averages = 4, T1delay=8 sec.

Segmentation of the striatum and thalamus was performed manually on the T2-weighted anatomical MR images, and ROIs were overlaid on the GluCEST maps. The GluCEST contrast is measured as the asymmetry between an image obtained with saturation at the resonant frequency of exchangeable amine protons (+3 ppm downfield from water for glutamate), and an image with saturation equidistant upfield from water (−3 ppm), according to the following equation:

$$GluCEST_{asym(\Delta\omega=3ppm)} = \frac{M_{sat(-3ppm)} - M_{sat(3ppm)}}{M_{sat(-3ppm)}} * 100 \quad \text{(Eq. 1)}$$

where M_{sat} (±3ppm) are the magnetizations obtained with saturation at a ‘3’ and ‘–3’ ppm offset from the water resonance.

Radiofrequency field inhomogeneity (B_1) and static magnetic field inhomogeneity (B_0) in the brain slice were corrected using B_1 and B_0 maps generated from the same slice. The B_0 map was calculated by linearly fitting the accumulated phase per pixel following phase unwrapping against the echo time differences from GRE images collected at varying TE = 3.5, 4.0, and 4.5 ms. B_1 maps were calculated from two images acquired using square preparation pulses with flip angles 30° and 60° (pulse duration = 65 μs, averages = 2) followed by a spoiler gradient. A flip angle map was generated, and a linear correction for B_1 was calculated as a ratio of the actual B_1 to the expected value.

We started the study with higher number of animals in both the groups (control = 14, MPTP = 18) expecting there would be deaths related to the neurotoxicity in the group, but there was no treatment related death. Due to the sudden head movement during the MR acquisitions, data from some of the animals had to be excluded in the post processing owing to large B0 and B1 inhomogeneity artifacts in the GluCEST results, leading to a reported number of the mice in each group, i.e. control = 11 and MPTP = 13.

Immunohistochemical analysis of brain

A sub-set of mice was prepared for immunohistochemistry (IHC): MPTP treated (n=7) and control PBS treated (n=5). After imaging, the mice were sacrificed using a standard method of transcardial perfusion/fixation with 10 ml of phosphate buffered saline (PBS) followed by 20 ml of 10% formalin. The brains were removed from the skull and stored overnight at 4°C in 10% formalin. Paraffin-embedded sections were sliced at 6 μm thickness, and mounted on poly-lysine coated slides.

Several protocols for IHC were performed utilizing peroxide and streptavidin-biotin pretreatments, and a horseradish peroxidase developing system (†BioGenex, Hyderabad, AP India) or the ABC system by Abcam (‡).The primary antibodies used in this study include tyrosine hydroxylase (TH, RbTH UPN88, Millipore, †) which is specific for dopaminergic neurons, VGLUT1 (pre-synaptic vesicular glutamate transporter protein, Synaptic Systems), and glial fibrillary acidic protein (GFAP ‡) to monitor the glial cell response. VGLUT1 slides were also subjected to microwave pre-treatment for 15 minutes at 100°C in citrate buffer (Vector Antigen Unmasking Solution, Vector Laboratories). VGLUT1 and GFAP immunostained slides were counterstained with hematoxylin.

Stained slides were scanned using an automatic slide scanner (Lamina Scanner, PerkinElmer). Scanned slides were viewed using CaseViewer (Histech, v1.3.0.41885). Quantification methods were performed in ImageJ (NIH) and averaged over the left and right hemispheres for all antibodies. The mean intensity of TH immunostaining in the striatum was quantified from square ROIs segmented from 3.5× images. ROIs from the color image (without counterstain) were converted to gray-level intensity for quantification. In the SNc, the punctate dark-brown stain was selected using a fixed threshold for all mice, and the percent area occupied (%AOC) was calculated over a square ROI cropped from 10× images.

In order to quantify VGLUT1 and GFAP immunostaining, 3.5× images from the striatum were analyzed by the color deconvolution plug-in using the H-DAB color optical densities provided (Ruifrok & Johnston 2001). ROIs from the color image were converted to gray-level intensity for quantification. ROIs in GFAP images were selected over the entire striatum from the counter-stained image and applied to the brown image. A consistent threshold was applied, and the %AOC by GFAP immunostaining was calculated. Due to very low threshold, for the measurement of GFAP positive pixels in the motor cortex region, manual counting was performed in the whole motor cortical region in the slice.

Statistical Analyses

For all results, a two-tailed non-equal variance Student’s t-test was used to compare results from MPTP treated with control mice. A significance level of at least $p \leq 0.05$ was determined using the Bonferroni correction. Mean values are reported and graphed, where error bars represent the standard deviation. Partial correlation analysis was used to explore the relationship among GluCEST data and motor function.

Results

MPTP exposure causes motor function deregulation

Treatment with MPTP did not cause any alteration in the weight of mice ($p > 0.61$). During the administration of MPTP to mice there was a significant reduction in the fore paw grip strength (Day 0: 1331 ± 167 g.sec, Day 8: 856 ± 211 g.sec; $p \leq 0.001$) while it was unchanged in the control mice (Day 0: 1336 ± 237 g.sec, Day 8: 1313 ± 234 g.sec; $p=0.80$, Fig 1a). Additionally, four limb hanging test results were found to be significantly reduced in mice treated with MPTP on Day 8 (32.1 ± 11.3 N.sec) compared to control mice (55.8 ± 11.9 N.sec, $p \leq 0.001$, Fig 1b).

MPTP leads to loss of SNc and striatal dopaminergic neurons

In the SNc, the intensity of TH immunostaining was reduced by 32.4 % in MPTP treated mice (%AOC; Control: 4.39 ± 0.91, MPTP: 2.96 ± 0.99, $p \leq 0.01$, Fig 1c). The mean intensity of TH immunostaining was further reduced by 22.4% in the striatum (%AOC: Control: 106.9 ± 11.8%, MPTP: 82.9 ± 11.7%, $p \leq 0.001$, Fig 1d) indicating a loss of dopaminergic innervations due to a loss of dopaminergic neurons in the striatum.

Elevation of glutamate in the striatum by ^{1}H MRS

Analysis of ^{1}H MR spectra using LCModel showed a significant increase in the level of striatal glutamate (Control 12.6 ± 1.7 mM vs MPTP 14.8 ± 2.6 mM; $p = 0.003$), GABA (Control 2.9 ± 0.6 mM vs MPTP 3.5 ± 0.8 mM; $p = 0.017$), and Gln (Control 5.5 ± 1.4 mM vs MPTP 7.0 ± 2.9 mM; $p = 0.022$) following MPTP treatment. There was no alteration in the levels of striatal NAA, Cre, Ins and choline in the MPTP group. The changes in the Glu, GABA and Gln were statistically significant. Under the experimental conditions used, Gln does not exhibit GluCEST effect and the change in GABA level is only 0.6 mM and it is expected to contribute to GluCEST.

GluCEST MRI of striatum, motor cortex and thalamus

GluCEST contrast was measured as the asymmetry between an image obtained with saturation at the resonant frequency of exchangeable amine protons (+3 ppm), and an image with saturation equidistant upfield from water (−3 ppm) (Eq. 1). ROIs for the GluCEST measurement in the striatum, motor cortex and thalamus were manually drawn on 2 mm thick coronal slice of T2 weighted images (Fig 3a,b). GluCEST imaging clearly showed elevated glutamate-dependent signal changes in the striatum of MPTP mice (Control: 23.3 ± 1.5 %, n=11; MPTP: 26.3 ± 1.1 %, n=13; $p \leq 0.001$; Fig 3c,d). Interestingly, elevated GluCEST in the motor cortex was also observed in the MPTP group (Control: 23.9 ± 1.3 %, n=11; MPTP: 26.3 ± 1.5 %, n=13; $p \leq 0.001$, Fig 3e,f). In contrast to the striatum and motor cortex, the average GluCEST contrast in the thalamus remained unaltered in MPTP and control mice (Control: 25.0 ± 1.8, MPTP: 26.2 ± 2.5; $p = 0.34$, Fig 3g,h).

VGLUT1 and GFAP immunohistochemistry

GFAP immunostaining was found to be elevated locally in the striatum (%AOC; Control: 1.5 ± 2.5, n=5; MPTP: 7.8 ± 1.8, n = 7; $p \leq 0.001$, Fig 4a,b), while VGLUT1 staining was

reduced by ~10% (Control: 102.2 ± 7.4, n=5; MPTP: 90.8 ± 7.9, n = 7; p≤0.05, Fig 4c). The MPTP exposure also led to elevated GFAP positive pixels in the motor cortex region of mice (Control: 8.0 ± 5.9, n=4; MPTP: 41.3 ± 18.6 number of positive pixels/slice, n=7; p=0.0006).

Correlation between GluCEST contrast and Motor function

Performance on the four-limb hanging test correlated negatively with GluCEST measurements in the striatum (R = −0.705, p=0.0001, n = 24, Fig 5a) and motor cortex (R = −0.617, p<0.001, n 24, Fig 5b), while the forepaw grip strength showed a negative association with GluCEST contrast in the striatum (R = −0.512, p=0.01, n = 24, Fig 5c) and motor cortex (R = −0.413, p<0.045, n = 24, Fig 5d), suggesting elevated glutamate in the striatum and motor cortex due to MPTP leads to motor function abnormality.

Association between GluCEST contrast and ^{1}HMRS derived glutamate

Compared to control animals, elevated GluCEST from the striatum of MPTP treated mice (Control: 23.3 ± 1.5 %, n=11; MPTP: 26.3 ± 1.1 %, n=13; p≤0.001) is positively associated with the changes in corresponding ^{1}H MRS derived glutamate levels (Control 12.6 ± 1.7 mM; MPTP 14.8 ± 2.6 mM; p = 0.0013).

Discussion

To the best of our knowledge, this is the first study to report *in vivo* imaging of elevated striatum glutamate levels caused by specific dopaminergic neuronal toxicity due to MPTP in the SNc. These results are corroborated ^{1}H MRS results showing elevated glutamate levels in the striatum of MPTP treated mice. This study also revealed elevated glutamate in the motor cortex. To our knowledge, this has not been reported previously. Elevated striatal and motor cortical glutamate levels were found to negatively correlate with motor function. Immunohistochemical analysis pointed towards astrogliosis to be the major cause of elevated glutamate levels in the striatum due to the drastic increase in the GFAP immunoreactivity in the striatum.

While previous ^{1}H MRS studies have shown elevated glutamate in the striatum of this model (Bagga *et al.* 2013, Chassain *et al.* 2013) 24 days post treatment of MPTP, there have been no imaging studies correlating the elevated glutamate levels with the astrogliosis detected within a very short time frame (2 days post 7 day MPTP treatment). In the striatum of control animals, the GluCEST asymmetry was found to be ~23%, with an intra-animal test-retest variability of less than 0.5 % and inter-animal variability ~ 1 % (data not shown). Considering the reported difference in the neuronal and glial contributions to glutamate (fraction of total glutamate localized in glia is ~15%) in the striatum (Tiwari *et al.* 2013), an estimated 3.5% of GluCEST contrast is derived from glial cells while the remaining 19.5% from neuronal glutamate. Assuming the distribution of glutamate in neurons and astroglia does not change 2 days following the end of the MPTP treatment, 10% reduction in the VGLUT1 will reduce the contribution of neuronal glutamate to ~17.8%. While remaining glutamate (8.5%; 26.3–17.8%) is localized in glial cells, showing ~2.4-fold increase in the glial contribution to total GluCEST, which is attributable to the increased number of glial

cells. Our histological data shows that while the striatal dopaminergic neurons are depleted in the MPTP mouse model, GFAP immunoreactivity in the MPTP group is increased by a factor of ~4, which can be attributed to the combination of increases in astroglial reactivity and number. This is also in agreement with previous studies, which showed increased number and size of astrocytes in the striatum followed by MPTP exposure (Tristao *et al.* 2014). Previous studies using the MPTP mouse model have shown a two-fold increase in glutamine synthetase (GS), which is also suspected to be caused by a proliferation of glial cells (Chassain et al. 2013). Most interestingly, ^{1}H MRS studies in striatum of late stage PD patients have shown no alteration in the level of glutamate or the combined glutamate-glutamine signal (Emir *et al.* 2012, Mazuel *et al.* 2015), while acute MPTP toxicity, mimicking an early stage of disease, leads to elevated glutamate pointing towards a temporary glial response to the loss of dopaminergic neurons in the striatum. Although, subchronic exposure to MPTP leads to reduction in the extracellular glutamate levels (Holmer *et al.* 2005, Holmer *et al.* 2005), we have found elevated GluCEST signal. This is due the fact that the GluCEST MRI and ^{1}H MRS measure the total glutamate in the brain which is mostly intracellular (Danbolt, 2001). Hence, the reported reduction of extracellular glutamate following MPTP exposure in mice will have a minimal effect in our study.

A novel finding in this study was of elevated GluCEST in the motor cortex as well as in striatum. Elevated GluCEST in the motor cortex and striatum may be linked to the presence of the axonal connectivity between the two regions via the motor pathway (Oh *et al.* 2014). Further investigations are needed to establish the root cause of this finding. The observed inverse correlation of GluCEST in both motor cortex and striatum with motor function suggests that these changes are functionally significant.

Increased GluCEST contrast provides the first non-invasive method for visualizing the spatial selectivity of astrogliosis *in vivo*. Lack of significant GluCEST changes in the thalamus suggests that GluCEST is able to distinguish specific regions of the brain where glutamate alterations occur. In the MPTP mouse model, high GluCEST contrast correlates with loss of four-limb strength, and is positively associated with the increased glutamate measured by ^{1}H MRS and immunochemical markers in the striatum. By way of contrast, a reduction in GluCEST contrast was recently reported following ciliary neurotrophic factor (CNTF) injection in the brain (Carrillo-de Sauvage *et al.* 2015). The reduced GluCEST contrast was attributed to astroglial hypertrophy as well as reduced cellular activity and reduction in the level of glutamine, a precursor for glutamate. The study also showed reduction in the NAA level, a marker for neuronal viability and health, suggesting the finding of reduced GluCEST is due to subduing of neuronal metabolism cause by CNTF. While further experiments are needed to fully elucidate the relationship between GluCEST and astroglial changes, it does appear that elevated GluCEST contrast correlated well with increased glutamate in MPTP model of dopamine deficiency.

GluCEST imaging technique can be readily translated to the clinical setting as shown by a recent study in human patients with epilepsy (Davis et al. 2015) and it can be potentially applied to the evaluation of a broad range of neuropathologies.

Conclusions

This is a first study to demonstrate application of GluCEST MRI technique in vivo to measure elevated level of glutamate in the MPTP model of dopamine deficiency. Changes in GluCEST results are positively associated with those from the ^{1}H MRS and immunohistochemical analysis. Immunohistology pointed towards astrogliosis as a cause of elevated glutamate in the striatum. Additionally, GluCEST in striatum and motor cortex was found to correlate negatively with the motor function suggesting a role of elevated glutamate in the regions in cerebral motor control, allowing application of GluCEST MRI as a tool to measure motor function *in vivo*.

Acknowledgments

This project was supported by the National Institute of Biomedical Imaging and Bioengineering of the National Institutes of Health through Grant Number P41-EB015893 and the National Institute of Neurological Disorders and Stroke through Award Number R01NS087516.

Abbreviations

Glu	Glutamate
Gln	Glutamine
GABA	γ–amino butyric acid
GFAP	Glial Fibrillary Acidic Protein
TH	Tyrosine Hydroxylase
MPTP	1-methyl-4-phenyl1,2,3,6-tetrahydropyridine
GluCEST MRI	Glutamate Chemical Exchange Saturation Transfer MRI
VGLUT1	vesicular glutamate transporter 1
NAA	N-Acetyl aspartate
Cre	Creatine
PD	Parkinson’s disease
SNc	Substantia nigra pars compacta
MRS	Magnetic Resonance Spectroscopy
PRESS	Point RESolved Spectroscopy
IHC	Immunohistochemistry
Tau	Taurine

References

Alexander GE. Basal ganglia-thalamocortical circuits: their role in control of movements. J Clin Neurophysiol. 1994; 11:420–431. [PubMed: 7962489]

Bagga P, Chugani AN, Varadarajan KS, Patel AB. In vivo NMR studies of regional cerebral energetics in MPTP model of Parkinson's disease: recovery of cerebral metabolism with acute levodopa treatment. Journal of neurochemistry. 2013; 127:365–377. [PubMed: 23957451]

Bagga P, Patel AB. Regional cerebral metabolism in mouse under chronic manganese exposure: implications for manganism. Neurochem Int. 2012; 60:177–185. [PubMed: 22107705]

Cai K, Haris M, Singh A, Kogan F, Greenberg JH, Hariharan H, Detre JA, Reddy R. Magnetic resonance imaging of glutamate. Nature medicine. 2012; 18:302–306.

Carrillo-de Sauvage MA, Flament J, Bramoulle Y, et al. The neuroprotective agent CNTF decreases neuronal metabolites in the rat striatum: an in vivo multimodal magnetic resonance imaging study. J Cereb Blood Flow Metab. 2015; 35:917–921. [PubMed: 25833344]

Chassain C, Bielicki G, Carcenac C, Ronsin AC, Renou JP, Savasta M, Durif F. Does MPTP intoxication in mice induce metabolite changes in the nucleus accumbens? A (1)H nuclear MRS study. NMR in biomedicine. 2013; 26:336–347. [PubMed: 23059905]

Crescenzi R, DeBrosse C, Nanga RP, et al. In vivo measurement of glutamate loss is associated with synapse loss in a mouse model of tauopathy. NeuroImage. 2014; 101:185–192. [PubMed: 25003815]

Danbolt NC. Glutamate uptake. Prog Neuorbiol. 2001; 65:1–105.

Davis KA, Nanga RP, Das S, et al. Glutamate imaging (GluCEST) lateralizes epileptic foci in nonlesional temporal lobe epilepsy. Sci Transl Med. 2015; 7:309ra161.

Emir UE, Tuite PJ, Oz G. Elevated pontine and putamenal GABA levels in mild-moderate Parkinson disease detected by 7 tesla proton MRS. PLoS One. 2012; 7:e30918. [PubMed: 22295119]

Gazewood JD, Richards DR, Clebak K. Parkinson disease: an update. Am Fam Physician. 2013; 87:267–273. [PubMed: 23418798]

Gluck MR, Youngster SK, Ramsay RR, Singer TP, Nicklas WJ. Studies on the characterization of the inhibitory mechanism of 4′-alkylated 1-methyl-4-phenylpyridinium and phenylpyridine analogues in mitochondria and electron transport particles. Journal of neurochemistry. 1994; 63:655–661. [PubMed: 8035189]

Haris M, Nath K, Cai K, et al. Imaging of glutamate neurotransmitter alterations in Alzheimer's disease. NMR in biomedicine. 2013; 26:386–391. [PubMed: 23045158]

Hirsch EC, Hunot S. Neuroinflammation in Parkinson's disease: a target for neuroprotection? Lancet Neurol. 2009; 8:382–397. [PubMed: 19296921]

Holmer HK, Keyghobadi M, Moore C, Meshul CK. l-dopa induced reversal in striatal glutamate following partial depletion of nigrostriatal dopamine with 1-methyl-4-phenyl-1,2,3,6-tetrahydropyridine. Neuroscience. 2005; 136:333–41. [PubMed: 16198485]

Holmer HK, Keyghobadi M, Moore C, Menashe RA, Meshul CK. Dietary restriction affects striatal glutamate in the MPTP-induced mouse model of nigrostriatal degeneration. Synapse. 2005; 57:100–12. [PubMed: 15906381]

Hosaka Y, Yokota T, Miyagoe-Suzuki Y, Yuasa K, Imamura M, Matsuda R, Ikemoto T, Kameya S, Takeda S. Alpha1-syntrophin-deficient skeletal muscle exhibits hypertrophy and aberrant formation of neuromuscular junctions during regeneration. J Cell Biol. 2002; 158:1097–1107. [PubMed: 12221071]

Kogan F, Singh A, Debrosse C, Haris M, Cai K, Nanga RP, Elliott M, Hariharan H, Reddy R. Imaging of glutamate in the spinal cord using GluCEST. NeuroImage. 2013; 77:262–267. [PubMed: 23583425]

Kordower JH, Olanow CW, Dodiya HB, Chu Y, Beach TG, Adler CH, Halliday GM, Bartus RT. Disease duration and the integrity of the nigrostriatal system in Parkinson's disease. Brain. 2013; 136:2419–31. [PubMed: 23884810]

Mazuel L, Chassain C, Jean B, Pereira B, Cladiere A, Speziale C, Durif F. Proton MR Spectroscopy for Diagnosis and Evaluation of Treatment Efficacy in Parkinson Disease. Radiology. 2015; 142764

Obeso JA, Rodriguez-Oroz MC, Rodriguez M, Lanciego JL, Artieda J, Gonzalo N, Olanow CW. Pathophysiology of the basal ganglia in Parkinson's disease. Trends Neurosci. 2000; 23:S8–19. [PubMed: 11052215]

Oh SW, Harris JA, Ng L, et al. A mesoscale connectome of the mouse brain. Nature. 2014; 508:207–214. [PubMed: 24695228]

Provencher SW. Estimation of metabolite concentrations from localized in vivo proton NMR spectra. Magn Reson Med. 1993; 30:672–679. [PubMed: 8139448]

Ruifrok AC, Johnston DA. Quantification of histochemical staining by color deconvolution. Anal Quant Cytol Histol. 2001; 23:291–299. [PubMed: 11531144]

Scotcher KP, Irwin I, DeLanney LE, Langston JW, Di Monte D. Effects of 1-methyl-4-phenyl-1,2,3,6-tetrahydropyridine and 1-methyl-4-phenylpyridinium ion on ATP levels of mouse brain synaptosomes. Journal of neurochemistry. 1990; 54:1295–1301. [PubMed: 2313288]

Sedelis M, Hofele K, Auburger GW, Morgan S, Huston JP, Schwarting RK. MPTP susceptibility in the mouse: behavioral, neurochemical, and histological analysis of gender and strain differences. Behav Genet. 2000; 30:171–182. [PubMed: 11105391]

Tiwari V, Ambadipudi S, Patel AB. Glutamatergic and GABAergic TCA cycle and neurotransmitter cycling fluxes in different regions of mouse brain. J Cereb Blood Flow Metab. 2013; 33:1523–1531. [PubMed: 23838829]

Tristao FS, Amar M, Latrous I, Del-Bel EA, Prediger RD, Raisman-Vozari R. Evaluation of nigrostriatal neurodegeneration and neuroinflammation following repeated intranasal 1-methyl-4-phenyl-1,2,3,6-tetrahydropyridine (MPTP) administration in mice, an experimental model of Parkinson's disease. Neurotoxicity research. 2014; 25:24–32. [PubMed: 23690159]

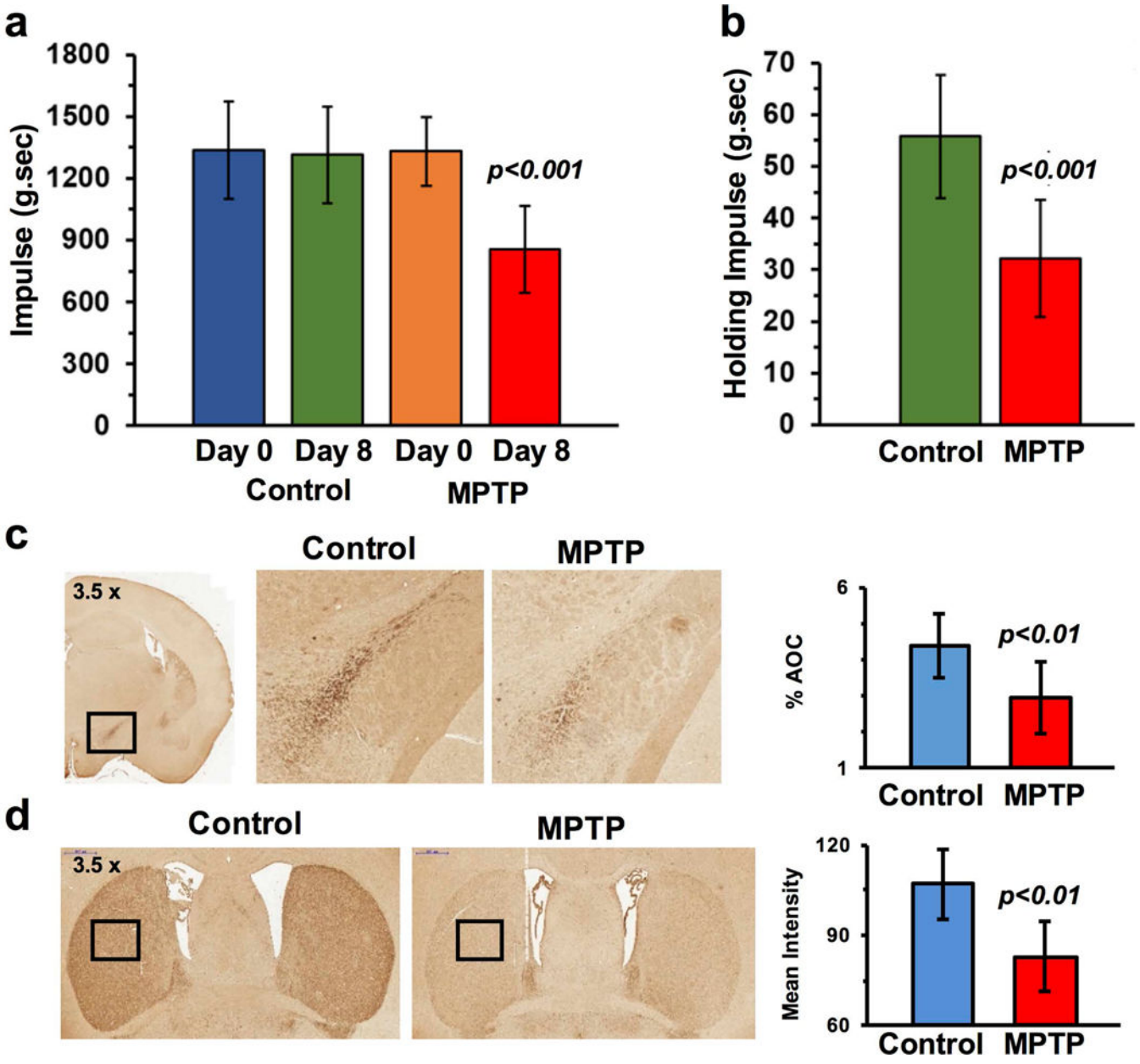

Figure 1.

Motor function and dopaminergic neuronal loss due to MPTP. (a) MPTP exposure led to a significant reduction in the forepaw grip strength and (b) four-limb hanging duration at 8th day from the start of MPTP treatment. (c) Tyrosine hydroxylase immunostaining results depicting severe loss of dopaminergic neurons in the substantia nigra pars compacta and (d) striatum following the treatment with MPTP in mice (bottom).

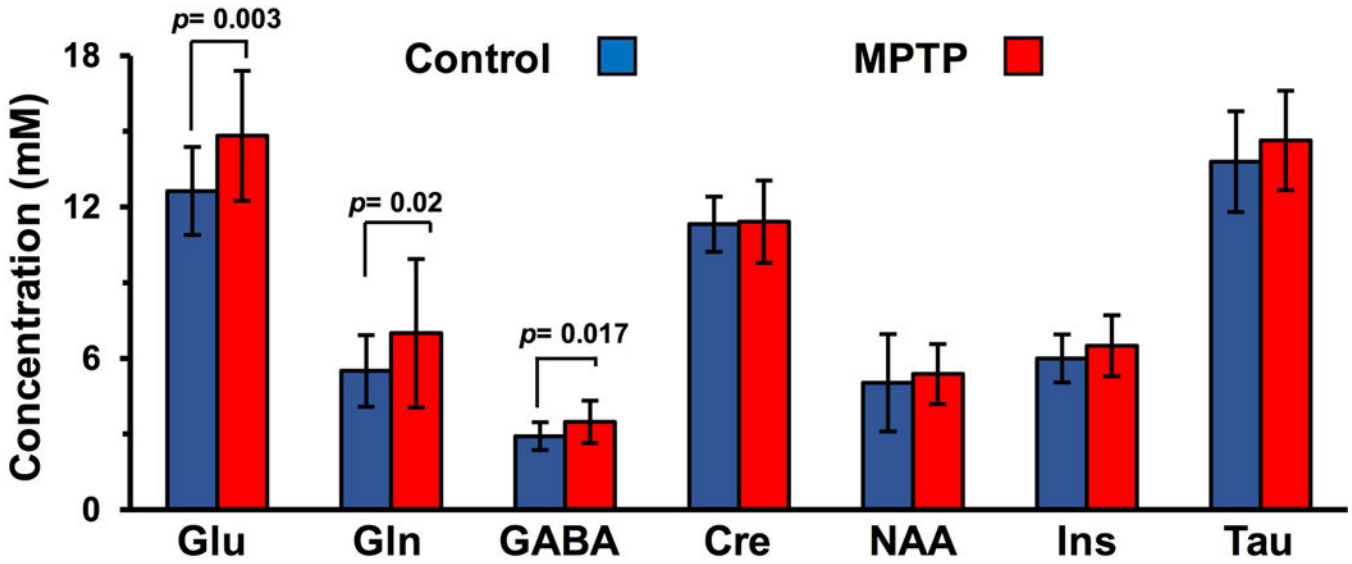

Figure 2.

Elevated glutamate in the striatum using ^{1}H MRS. ^{1}H MRS from striatum of control (blue) and MPTP treated (red) mice showing elevated level of glutamate (Control 12.6 ± 1.7 mM MPTP 14.8 ± 2.6 mM; p=0.0013), GABA (Control 2.9 ± 0.6 mM vs MPTP 3.5 ± 0.8 mM; p = 0.017), and Gln (Control 5.5 ± 1.4 mM vs MPTP 7.0 ± 2.9 mM; p = 0.022) following exposure to MPTP. Concentration (mM) of metabolites in striatum following MPTP treatment using LCModel. Glu Glutamate, Gln Glutamine, GABA γ–aminobutyric acid, Cr +PCr total creatine, NAA N-Acetylaspartate, Ins m-Inositol, Tau Taurine.

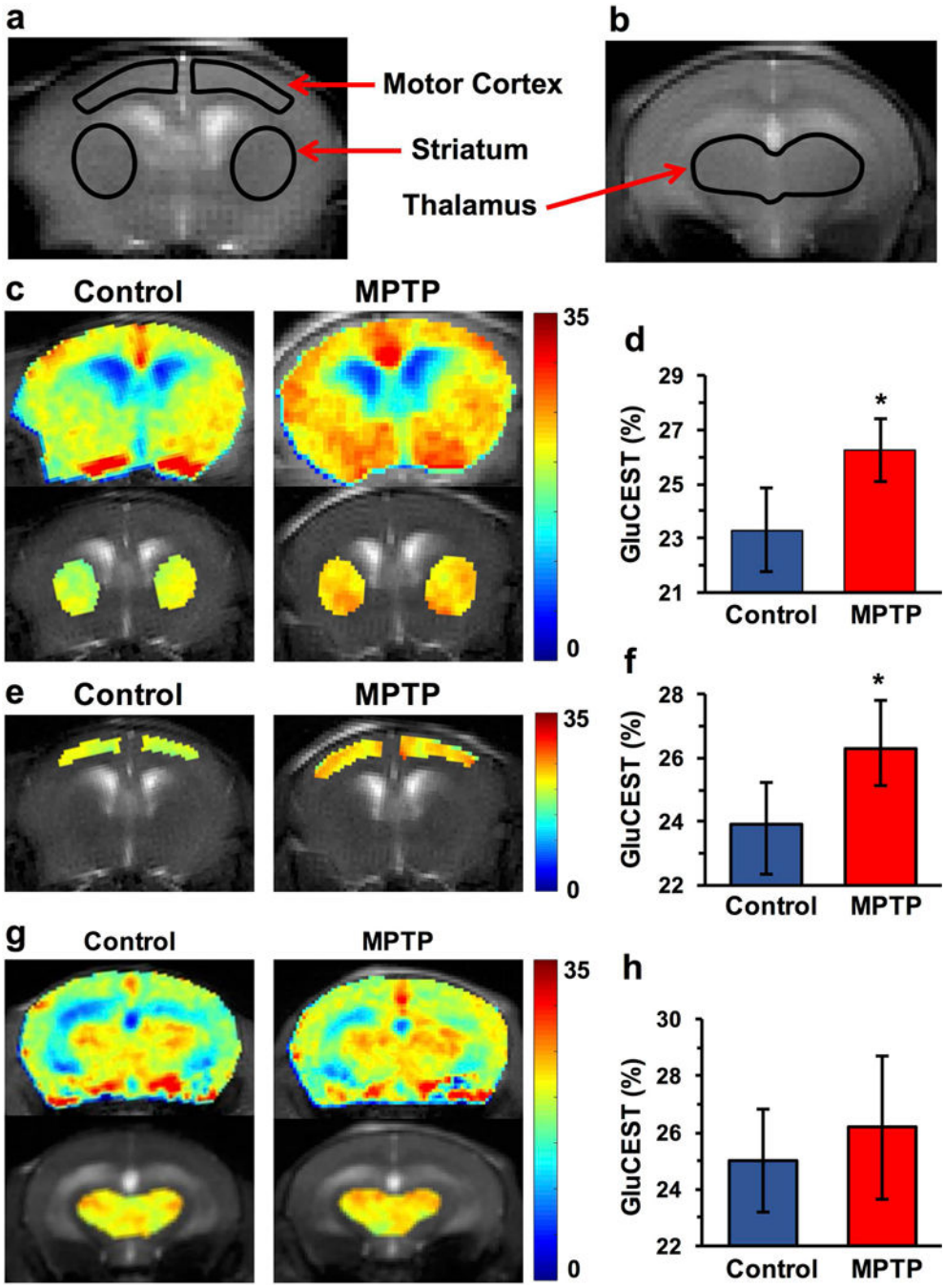

Figure 3.

GluCEST MRI following MPTP treatment. (a,b) T2 weighted images showing ROIs for striatum, motor cortex and thalamus in the coronal brain slices. (c,d) GluCEST contrast in the striatum showing higher GluCEST in MPTP (26.3 ± 1.1 %, n=13) compared to the control mice (23.3 ± 1.5 %, n=11; p≤0.001) (e,f) GluCEST map of motor cortex in the mouse brain showing higher GluCEST contrast in MPTP group (Control: 23.9 ± 1.3 %, n=11; MPTP: 26.3 ± 1.5 %, n=13; p≤0.001) while the (g,h) GluCEST contrast was unaltered

in the thalamus following MPTP exposure (Control: 24.8 ± 3.3, MPTP: 25.8 ± 3.4; p=0.34). *, p≤0.001

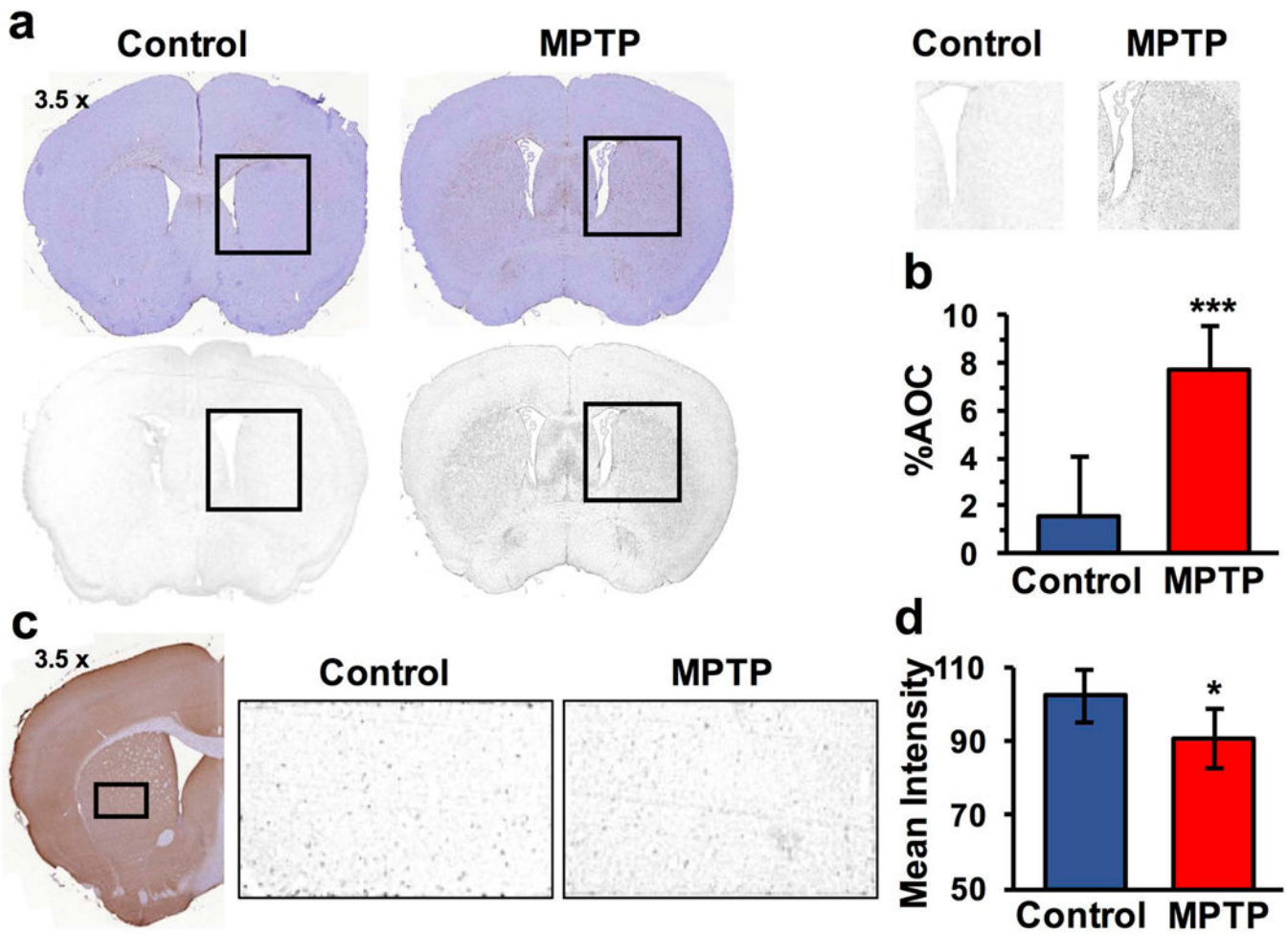

Figure 4.

Immunohistochemistry in striatum (a,b) GFAP immunoreactivity was found to be significantly increased in MPTP group (Control: 1.5 ± 2.5 %, n = 5; MPTP: 7.8 ± 1.8 %, n = 7; $p \leq 0.001$). (c,d) VGLUT1 staining was reduced by ~10% (Control: 102.2 ± 7.4 %, n = 5; MPTP: 90.8 ± 7.9 %, n = 7; $p \leq 0.05$).

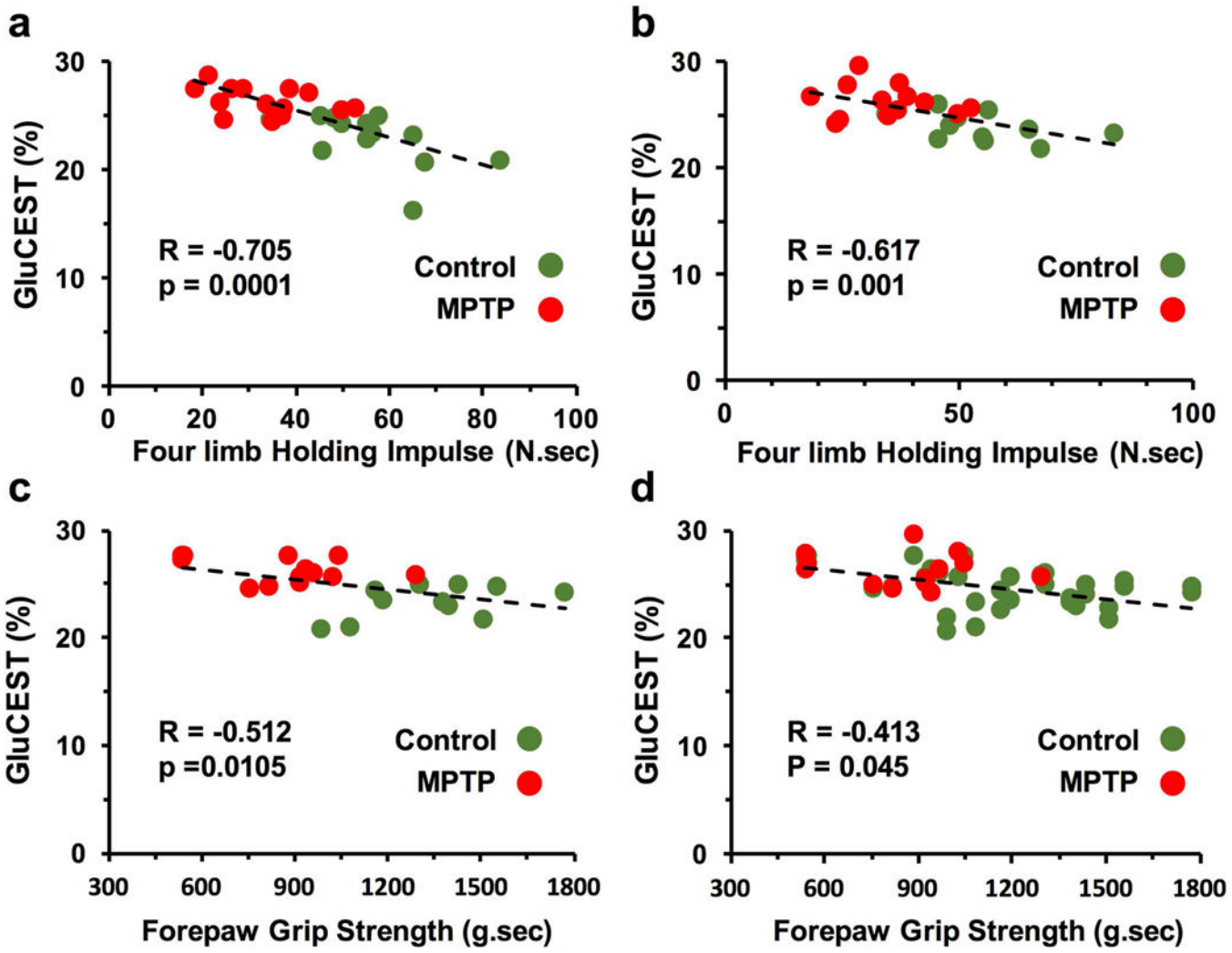

Figure 5.

Correlation plot of four-limb holding impulse with GluCEST in the striatum (a) and motor cortex (b) and forepaw grip strength with GluCEST in the striatum (c) and motor cortex (d) showing negative association between local glutamate level and motor function